Master's Thesis of Science

Investigation on Interaction between Colon Cancer Cells and Fibroblast using Patient-derived Organoid

오가노이드 모델을 이용한 대장암세포와 주변 섬유아세포의 상호작용에 대한 연구

August 2022

서울대학교 융합과학기술대학원
분자의학 및 바이오제약학과

김윤지

오가노이드 모델을 이용한 대장암세포와 주변 섬유아세포의 상호작용에 대한 연구

지도 교수 김 태 유

이 논문을 이학석사 학위논문으로 제출함
2022 년 7 월

서울대학교 융합과학기술대학원
분자의학 및 바이오제약학과
김 윤 지

김 윤 지의 이학석사 학위논문을 인준함
2022 년 7 월

위 원 장 _____ 강 경 훈 _____ (인)

부위원장 _____ 김 태 유 _____ (인)

위 원 _____ 이 유 진 _____ (인)

Investigation on Interaction between Colon Cancer Cells and Fibroblast using Patient-derived Organoid

By

Yun-Jee Kim

(Directed by Tae-You Kim, M.D., Ph.D.)

A thesis submitted in partial fulfillment of the requirements for the Degree of Master of Science

Department of Molecular Medicine and Biopharmaceutical Sciences
At Word Class University Graduated School or Convergence Science and Technology

July 2022

Chair GyeongHoon Kang (Seal)

Vice Chair TaeYou Kim (Seal)

Examiner Eugene C. Yi (Seal)

Abstract

Investigation on Interaction between Colon Cancer Cells and Fibroblast using Patient-derived Organoid

Yun-Jee Kim

Department of Molecular Medicine

And Biopharmaquetical Sciences

World Class University Graduate School

Of Convergence Science and Technology

Seoul National University

Cancer associated fibroblast (CAF) has been proposed as a main player in Tumor Microenvironment (TME) of solid tumors. It was demonstrated that two main subtypes of CAFs have supportive or suppressive influence on tumor cell through direct or indirect communication via paracrine factors or membrane receptor proteins[1]. These interactions allow tumor cells to acquire metastatic properties, immune escape, and drug resistance. Recent studies have focused on how two main subtypes of CAFs differentially regulate tumor microenvironment using mouse model or cell line. Additionally, colorectal cancer is known to onset with sequential genetic mutation. This can be the driving force at the beginning, and tumor microenvironment members such as CAF subpopulations and immune cells took a part in tumor-suppressive roles[2]. However, there is lack of explanation how tumor cells show uncontrolled malignant unlike normal cells. Patient derived organoids (PDO) have widely used owing to its advantageous feature in expectation of mimic the patient-specific tumor biology[3]. The present study focuses on how normal epithelial cell and tumor cell differentially response to stimulation under fibroblast coculture system.

Patient derived normal organoid, tumor organoid and fibroblast were well established and verified with expression of the cell type specific markers. Concordant results were also confirmed even after two types of cells were cultured together.

Direct coculture system was applied to monitoring both direct and in-direct cell to cell interaction between PDO and PDF. Nature of two types of cells were maintained after sorting. Normal organoid showed extensive phenotypic changes in response of CAF and NAF coculture such as increase in proliferation rate and more cystic morphology. On the other hand, tumor organoid did not show visible difference between mono-culture control and NAF/CAF coculture counterpart.

To discover the molecular mechanism involved in significant variance between responses of normal and tumor organoid, RNA-sequencing and further analyze with Gene Set Enrichment Analysis (GSEA). It was revealed that normal organoid showed extensive signaling pathways were up- or down- regulated when cultured with NAFs and CAFs. Unlike the normal organoids, tumor organoids showed fewer pathways were regulated by coculture of matched fibroblasts. Same results were shown also in organoids from another patient.

Altogether, in-vitro PDO and PDF 3D coculture system uncovered with a reflection of in-vivo tumor microenvironment. The difference in degree between normal and tumor organoid cultured with fibroblast might implicated that transcriptional mechanism involved in could be the biomarker.

Keyword: Colorectal Cancer, Tumor microenvironment, Patient-Derived Organoid, Patient-Derived fibroblast, Cancer associated fibroblast, Normal fibroblast.

Student Number: 2020-29330

Table of Contents

List of Tables

보존용 학위논문 정오표

페이지	정정 전	정정 후
p. i : 13	2	3
p. i : 17	3	2
p. 5 : 6	5,6	7,6
p. 5 : 9	7	5
p. 5 : 21	10	9
p. 6 : 20	14	15
p. 9 : 2	(3)	2

※ 본문의 캡션이 참고문헌 목록의 번호와 일치하지 않아 참고문헌 목록의 번호에 맞게 정정

Introduction

Cancer Associated Fibroblasts (CAF) is one of the most influential components in tumor microenvironment and has been extensively studied in various cancer types such as Colorectal Adenocarcinoma, Pancreas Ductal Adenocarcinoma, and prostate cancer[4]. There have been several studies that elucidate CAF have influence on tumor progression, metastasis, and immune infiltration[5,6]. During tumorigenesis, especially in CRC, loss of function-mutation of APC is considered as the first heat in early stage of tumor development via canonical WNT signaling pathway[7]. Addition to APC mutation, accumulation of further genetic mutations such as Kras, TP53 is also known as major players in CRC development. However, there is limitation in these genetic mutations to explain how tumor acquires their ability for further progression, metastasis, and drug resistance. CRC is known to interact with surrounding tumor microenvironment. Especially one of the consensus molecular subtypes (CMS), CMS4 CRC is marked by prominent stromal invasion[8]. This demonstrates the importance of tumor microenvironment and its component.

Under normal and homeostatic condition, it has been shown that the genes that are related to the epithelial-mesenchymal transition(EMT) are known as a regulator in differentiation[9] and wound healing process [10]. On the other hand, in the case of tumor microenvironment, CAFs provides tumor cell with cytokines that induce EMT signal in epithelial cells and allow tumor cell to acquire metastatic ability[11]. Furthermore, during differentiation stage of intestinal stem cell, balance between stemness promoted by Wnt, R-spondin and differentiation stimulation induced by BMP signaling pathway are accurately controlled and discriminate through the distribution of various fibroblast that secret different cytokines. Unlike normal stroma, stromal Hedgehog signaling pathway that produced mainly by CAFs are inhibited, leading to disruption of homeostasis, induction of uncontrolled stemness, and

hampered epithelial cell differentiation with function[6]. Lastly, Epithelial-stromal communication via cytokines has been considered as main causative of immune suppressive condition surrounding tumors[12]. Conventional epithelial cell-only culture system might not be sufficient to understand mechanism of tumorigenesis under tumor microenvironment which is composed of various cell types. Thus, there is an unmet need for a model system to study the epithelial-stromal interaction in vitro.

Like tumor microenvironment composed of more than one cell type, in the case of multicellular organism like human, the cells with various function interact with each other through paracrine or autocrine factors and this connection occurs in 3-Dimensional tissue. In other word, this spatial organization is important. Indeed, ECM components that mechanically support cells including epithelial cells not only provide physical scaffold, but also induce mechano-transduction within the cells, controlling the signaling pathway through binding to cell surface protein[13]. For these reasons, it is necessary to design in vitro 3D model system that resembles tissue. Organoid derived from tumor and adult stem cell has been widely utilized, which resemble normal tissue functional differentiation in vitro[14]. To be more specific, unlike conventional 2D cell culture using cancer cell line, which accumulates uncontrolled mutation during passaging, Patient Derived normal and tumor Organoids (PDOs) are advantageous as these cells could be cultured for extended time without change in their own properties (genetic background, drug response, morphology, etc.) one recent study uncovered molecular mechanism how liver cancer gains resistance to anti-cancer drug, such as 5-Flourouracil and sorafenib, by using organoid and fibroblast[15]. Patient-derived Xenograft (PDX) model is also known as model system that recapitulate Patient nature and tumor microenvironment. However, difference of epigenetic landscape between mouse and human might have influence on progression of the xenografted tumors[16]. Furthermore, mouse immune system that interacts with the patient derived tumor is not perfectly same with host immune itself. These suggest that PDO is suitable ex vivo model.

In the present study, coculture of patient derived organoids (218 normal organoid and 218 tumor organoid, 218nO and 218tO respectively) and matched fibroblast (218NAF and 218CAF) was conducted. Uncovering how normal colonic organoid and CRC counterpart differently response to stimulation from fibroblast might give insight to a novel biomarker to discriminate normal and tumor.

Materials and Methods

Antibodies

Rabbit monoclonal antibody recognizing Vimentin (5741) were purchased from Cell Signaling Technology. FITC anti-human CD326(324204) were purchased from Biolegend. Mouse monoclonal antibody recognizing FAP (H00002191-M01) was purchased from Abnova. Rabbit polyclonal antibody recognizing PDGFRα (SC-338) were purchased from Santa Cruz. Alexa Flour 594 goat anti-rabbit antibody(A11008), Alexa Flour 488 goat anti-mouse antibody(A11001) were obtained from Thermo Fisher Scientific.

Establishment of Patient-derived Organoids

Normal and tumor tissues were processed as described previously to establish PDOs with minor modifications (3). Firstly, crypts were isolated by cutting normal mucosa into 1-2 mm pieces and washing with Dulbecco's phosphate-buffered saline (DPBS) until there is no debris in supernatant. Normal colonic mucosal fragments were manually washed with 2mM ethylenediaminetetraacetic acid/ DPBS chelation buffer and were incubated on ice for 1h. Next, extraction of crypt is completed by shacking the tube vigorously after being washed with basal media composed of advanced DMEM/F12 (Invitrogen, Carlsbad, CA, USA) supplemented with penicillin/streptomycin (Invitrogen), 10 mM HEPES, and GlutaMAX (Invitrogen). In the case of tumor organoids, fresh tumor tissues were washed with DPBS and minced with gentle MACS Dissociator (Miltenyi Biotec, Bergisch Gladbach, Germany). The tissue pieces were filtered with a 70μm cell strainer to eliminate debris and washed with basal media. The isolated normal crypt and tumor cells pellets were mixed with Matrigel (Corning, NY, USA) in 12 well plates. Organoid medium was added after Matrigel being solidified at a 37˚C incubator. The composition of organoid medium is as follows. For normal organoid, 0.2nM recombinant wnt surrogate(Immunoprecise Antibiodies), 10% R-spondin1 CM, 100ng/ml recombinant Noggin(PeproTech, Cranbury, NJ, USA), 50ng/ml recombinant human EGF (PeproTech), B27 (Invitrogen), 1.25mM N-acetyl cysteine (Sigma-Aldrich, St. Louis, MO, USA), 10mM nicotinamide (Sigma), 3 μM SB202190 (Sigma), 500nM A83-01 (Tocris, Bristol, UK), 10nM prostaglandin E2 (Sigma), 10nM gastrin (Sigma), and 100μg/ml Primocin (InvivoGen, San Diego, CA, USA) in basal medium.

Establishment of Patient-derived Fibroblast and passaging

Patient derived fibroblast were extracted from matched normal and tumor respectively. Cancer-associated fibroblast in supernatant of digested tumor tissue was collected and cultured in fibroblast medium supplemented with penicillin/streptomycin (Invitrogen), GlutaMAX (Invitrogen), 10% FBS and MEM non-essential amino acid solution (Welgene). In the case of Normal associated fibroblast, the colonic mucosal fragments were further minced by gentleMACS Dissociator (Miltenyi Biotec, Bergisch Gladbach, Germany). The samples were filtered with a 70μM cell strainer for elimination of microscopic tissue debris. Collected cells were supplied with fibroblast medium. After recovery of fibroblast is confirmed, the fibroblasts were cultured twice in a week.

PDO culture and passaging

Organoid culture media was removed and added three times a week. Organoids were passaged once in a week and the duration of culture was varied according to their proliferation rate. Organoids embedded in Matrigel were collected and dissociated by mechanical disruption or by using Cultrex organoid harvesting solution (R&D systems) and then incubated on ice for 45 min. The remaining Matrigel was washed out with cold DPBS and cells were dissociated with Accutase (Stem Cell Technologies, Canada). After further washing with DPBS, cells were seeded with Matrigel. Only organoids with passage under 15 times were used.

Organoid and fibroblast coculture

Coculture was conducted by directly mixing fibroblast and organoid in Matrigel with the ratio of 1:2. After 3 days of coculture, organoids were separated from fibroblast by centrifugal force difference between organoid and fibroblast.

Immunofluorescence and EdU incorporation assay

For immunofluorescence (IF), organoids were fixed with 3.7% formaldehyde for 15 min at room temperature. After washing with 0.1% BSA in PBS for 3 times, 0.2% Triton X-100 (Sigma) was used for permeabilization for 15min at room temperature. After 1h of blocking with 4% BSA solution, primary antibodies were added with a sufficient dilution ratio and incubated for overnight at 4°C. Then secondary antibody tagged with desired fluorescence were added and then detected. EdU incorporation assay was carried out using the Click-iT Plus EdU Alexa Fluor 594 Imaging Kit (Life Technologies), 10uM of EdU was added into organoid and incubated at least 4 hours. EdU reaction cocktail was added following manufacturer's instruction. After 30min of incubation, DNA was stained, and the samples were detected.

For IF of fibroblasts, the cells were seeded on Poly-L-Lysine (Sigma) coated a cover glass for three days. After being washed with PBS, cells were fixed with 3.7% formaldehyde for 15 min on ice. Cells were further washed and permeabilized in 0.25% Triton-X100(Sigma). Cells were incubated at room temperature with 2% BSA blocking buffer. After additional washing, cells were incubated with desired primary antibodies overnight at 4°C. Cells were incubated with Secondary Antibodies for 1 hour at room temperature with florescence if needed.

RNA extraction and RNA-seq

Total RNAs were extracted from organoids after 3 days of coculture. Total RNA was extracted with TRI reagent (Molecular Research Center, #TR-118) following manufacturer's instruction. Total RNA was further processed and reverse transcribed to synthesize cDNA Real-time qPCR (RT-qPCR) was performed as previously described. Primer sequences used for RT-qPCR are described in Table 1. Sequencing libraries were prepared following the standard protocol of Illumina Inc. for high-throughput sequencing. The transcriptome was subsequently sequenced with a Genome Analyzer IIX (Illumina Inc.) as previously described[17]. Sequenced reads were aligned to human transcript following the UCSC database (Homo_sapiens.GR37/hg19) for expression analysis.

Bioinformatics Analysis

RNA-seq data of 6 differentially expressed gene cluster sets was subject to the Gene Set Enrichment Analysis following to the GSEA user manual[18]. GSEA was operated against Gene Ontology, Hallmarks, KEGG pathway gene sets using default parameters.

Table 1. Primer sequences used in the cell type validation via RT-qPCR

Gene	Sequence
EPCAM_F	GCCAGTGTACTTCAGTTGGTGC
EPCAM_R	CCCTTCAGGTTTTGCTCTTCTCC
CDH1_F	GTGTATGTGGCAATGCGTTC
CDH1_R	TGCCCACAAAATGAAAAAGG
ACTA2_F	GTGTTGCCCCTGAAGAGCAT
ACTA2_R	GCTGGGACATTGAAAGTCTCA
FAP_F	ATGAGCTTCCTCGTCCAATTCA
FAP_R	AGACCACCAGAGAGCATATTTTG
VIM_F	ACCAACGACAAAGCCCGCGT
VIM_R	CAGAGACGCATTGTCAACATCCTGT

Table 2. Primer sequences used in RNA-sequencing validation via RT-qPCR

Gene	Sequence
ITGB4_mRNA_F	CCCCCTTCTCCTTCAAGAAC
ITGB4_mRNA_R	GCTGACTCGGTGGAGAAGAC
CXCL16_mRNA_F	CTGGCCATCATCTTCATCCT
CXCL16_mRNA_R	GAGTCCGTCTCCTCACAAGC
FYN_mRNA_F	TGGGGAAGTATGGATGGGTA
FYN_mRNA_R	CACCACTGCATAGAGCTGGA
F3_mRNA_F	GGGCTGACTTCAATCCATGT
F3_mRNA_R	GAAGGTGCCCAGAATACCAA

Results

Patient derived Organoids and matched fibroblasts retain the cell type specific markers

Firstly, to characterize the two mainly used cell types in this study, cell type specific markers are verified by immunofluorescence and RT-qPCR. In the case of patient derived organoid (hereafter PDO) expressed epithelial cell type specific marker *EPCAM* (Figure 1A). On the other hand, Patient derived fibroblasts (hereafter PDF) showed *VIM*, *FAP*, *PDGFRA* expression (figure 1B). RT-qPCR showed concordant results. There was *ACTA2* expression in PDF exclusively and there was no EPCAM mRNA expression in PDF, not like in PDO (Figure 1C).

To establish ex-vivo3D model system mimicking tumor microenvironment, three types of coculture methods could be conducted (Figure 1D). Each of methods has its own pros and cons. Direct coculture let fibroblast and cancer cell interact both directly and indirectly through soluble factor. However, there are always limited fibroblast due to their slower cell devision. Also, it is hard to detect organoid epxression changes only unless it is sorted. The other two methods are free from limitation of fibroblast abundancy and separation. However, these two methods can only detect in direct cell interaction through growth factor, chemokine, hormones etc. It is hard to study direct cell to cell interaction through these methods. For these reasons, direct mixture of PDFs and PDOs were used as a coculture condition.

(A)

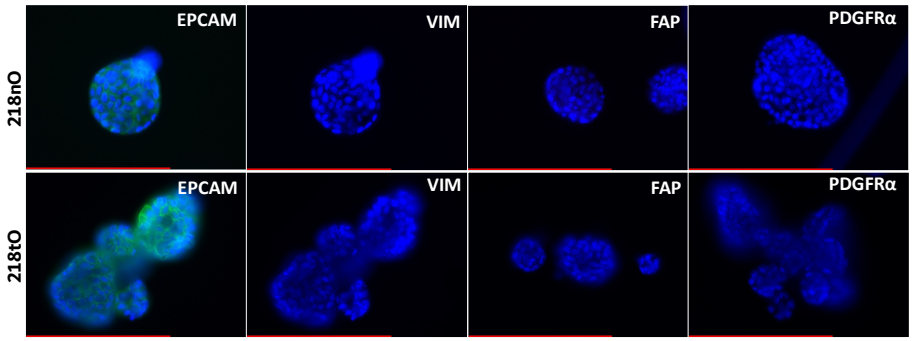
218nO
218tO
EPCAM
VIM
FAP
PDGFRα

(B)

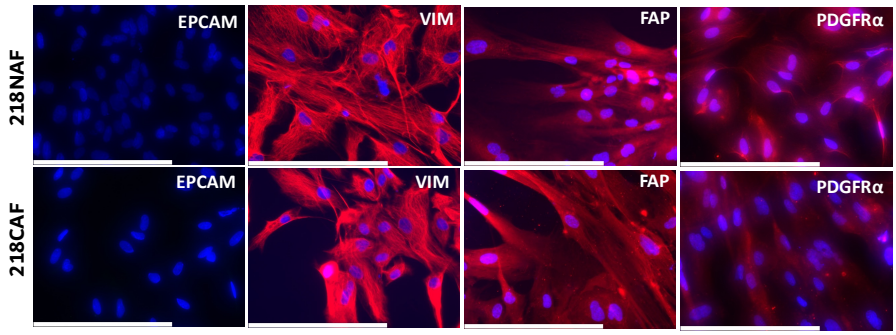
218NAF
218CAF
EPCAM
VIM
FAP
PDGFRα

(C)

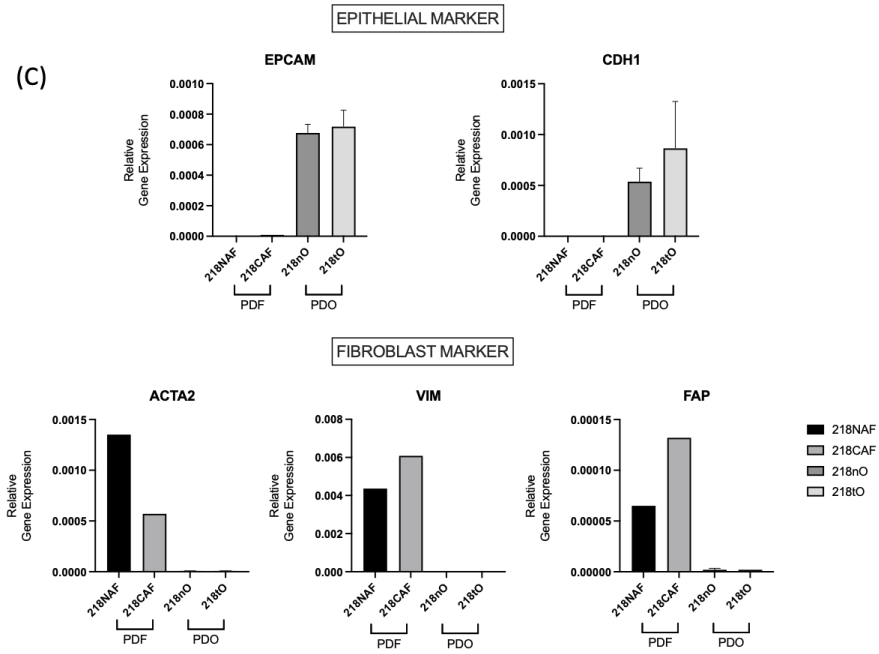
EPITHELIAL MARKER
EPCAM
CDH1
Relative Gene Expression
218NAF
218CAF
218nO
218tO
PDF
PDO
FIBROBLAST MARKER
ACTA2
VIM
FAP
218NAF
218CAF
218nO
218tO

(D)

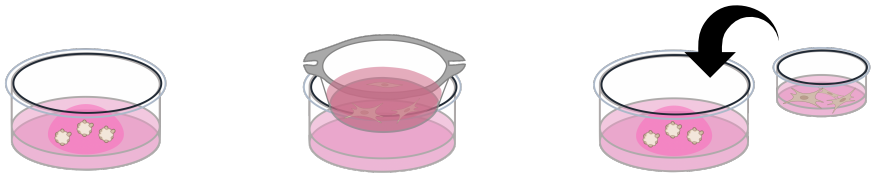

	Direct Co-culture	Indirect Co-culture	Fibroblast Conditioned Media
Cell to Cell Direct Interaction	✓	✗	✗
Soluble Factor	✓	✓	✓
No need of Fibroblast	✗	✗	✓
No need for separation	✗	✓	✓

Figure 1. The cell type-specific markers confer Patient-derived cells were retain their own markers.

(A) Immunofluorescence analysis of 218nO (Top) and 218tO (Bottom) stained with *EPCAM*, Vimentin (*VIM*), *FAP* and *PDGFRA* (scale bar=200μm).

(B) Immunofluorescence analysis of 218NAF (Top) and 218CAF, stained with *EPCAM, VIM, FAP* and *PDGFRA* (Bottom) (scale bar=200μm).

(C) Real-Time qPCR was conducted with primers targeting *EPCAM, CDH1, ACTA2, VIM, FAP* and were normalized to 18S ribosomal. BAR represent the mean SD of two independent biological samples.

(D) Schematic view of three types of coculture.

Normal organoid and Tumor organoid show different phenotypic response upon their matched fibroblast coculture

To figure out whether the PDOs were affected by PDF, normal and tumor organoids were cultured with normal associated fibroblast (NAF) or cancer associated fibroblast (CAF) at a 1:2 ratio for 3 days. Morphological changes might imply that there were genetic or epigenetic fluctuation under coculture condition. There were 2 major changes in phenotypes of PDO (Figure 2A). Firstly, normal organoids cultured with NAF or CAF showed extended diameter comparing to mono-cultured control. On the other hand, matched tumor organoid did not show this change. In addition to its size, cystic morphology was dramatically shown in normal organoid cultured with matched fibroblasts. Tumor organoid did not show distinct morphology change. In summary, PDO cultured with its matched PDF showed more cystic and extended diameter comparing to one without PDF, and this is the only case for normal organoid, not tumor organoids.

Decreased in branching morphology and increase in size were confirmed in the prior experiments. According to the prior research, in the process of regeneration of normal intestinal tissue, fibroblasts promote epithelial cells to proliferate. In terms of cell proliferation, at day 3 of coculture, EdU proliferation assay was conducted to measure and compare the cell growth between mono and cocultured organoids. Indeed, normal organoids with fibroblasts showed increased in EdU positive cells, implying that organoids proliferates more rapidly than organoids cultured without fibroblasts (Figure 2B). In the case of tumor organoids, there was no difference in proliferation rate between cocultured and monocultured organoids (Figure 2C). To rule out the probability of fibroblast contamination, cell tracker was used. Those two cell types were stained with different color and thus it is possible to distinguish each cell type and organoid-only expansion. In the

coculture context, normal organoid stained with green showed expansion and tumor organoids did not (Figure 2D, 2E).

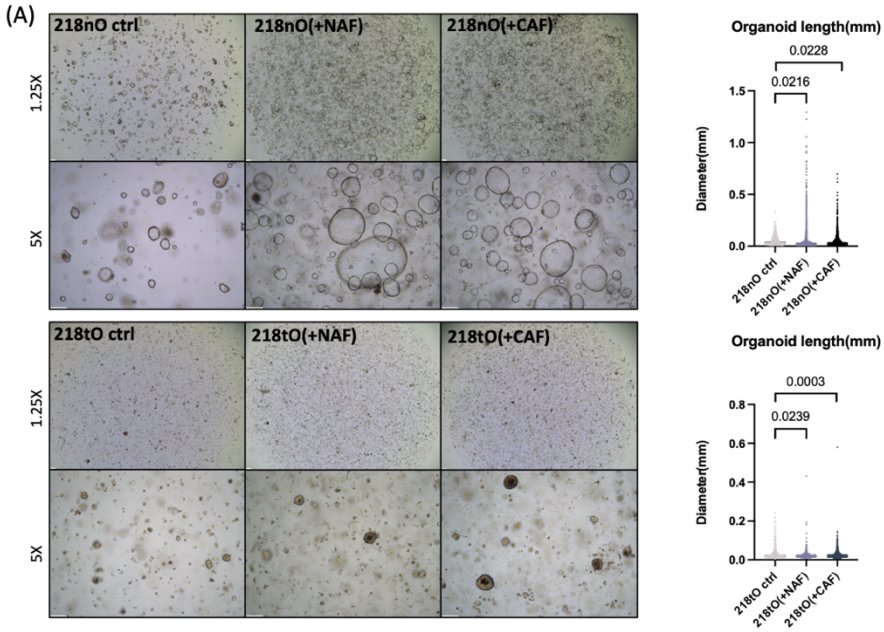

(B)

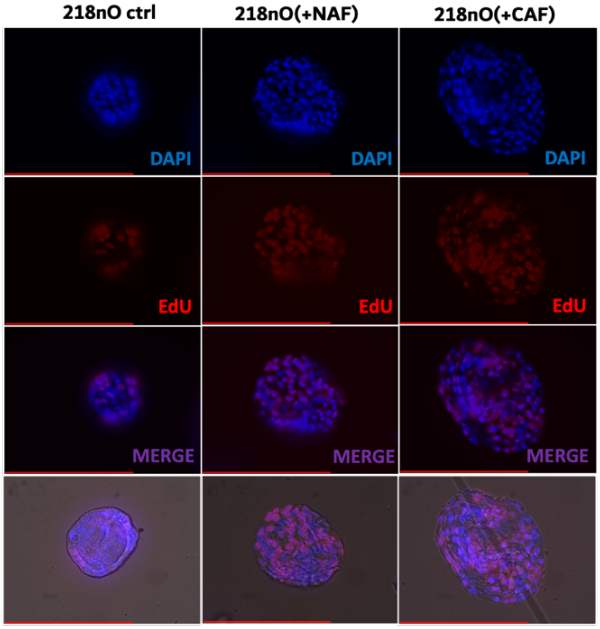
218nO ctrl
218nO(+NAF)
218nO(+CAF)
DAPI
EdU
MERGE

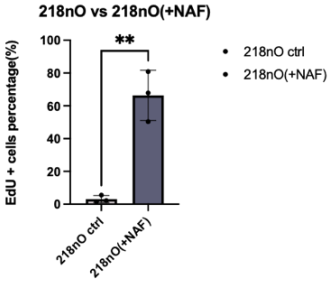
218nO vs 218nO(+NAF)
EdU + cells percentage(%)
100
80
60
40
20
0
**
218nO ctrl
218nO(+NAF)

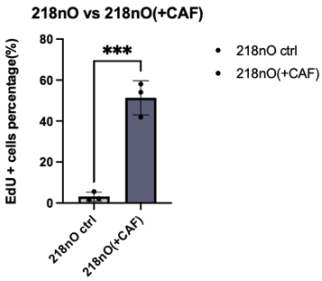
218nO vs 218nO(+CAF)
EdU + cells percentage(%)
80
60
40
20
0
***
218nO ctrl
218nO(+CAF)

(C)

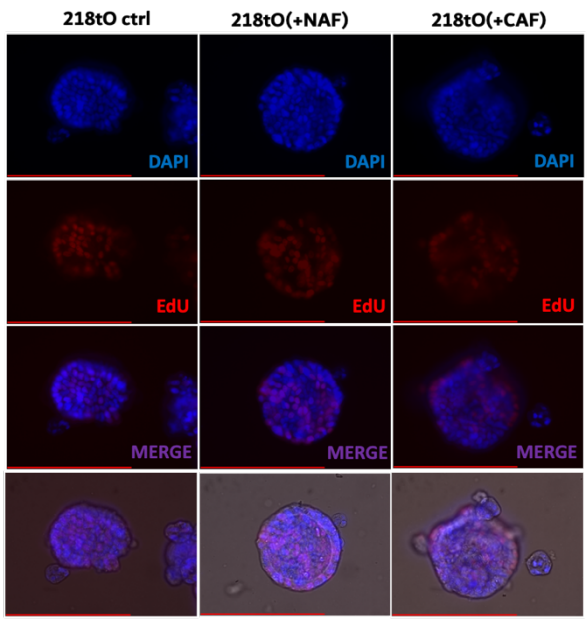
218tO ctrl
218tO(+NAF)
218tO(+CAF)
DAPI
EdU
MERGE

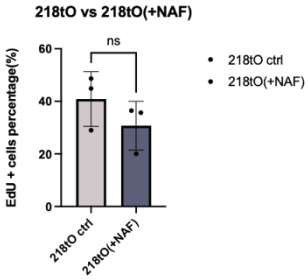
218tO vs 218tO(+NAF)
EdU + cells percentage(%)
60
40
20
0
ns
218tO ctrl
218tO(+NAF)

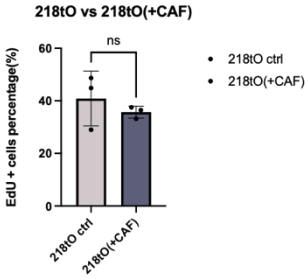
218tO vs 218tO(+CAF)
EdU + cells percentage(%)
60
40
20
0
ns
218tO ctrl
218tO(+CAF)

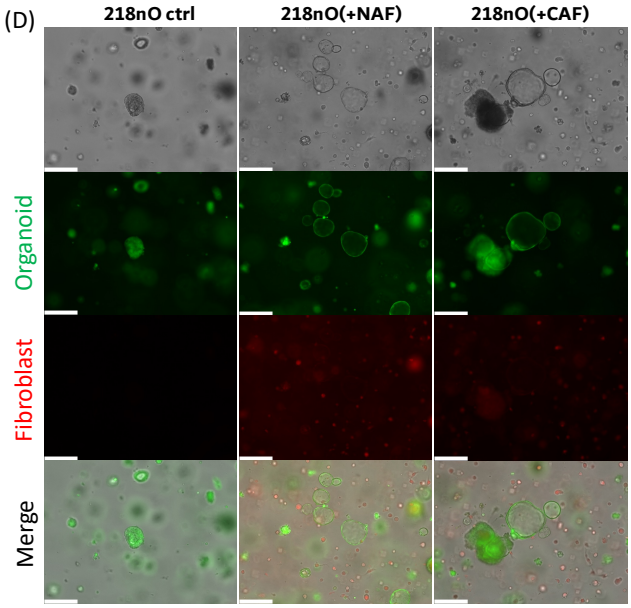
(D)
218nO ctrl
218nO(+NAF)
218nO(+CAF)
Organoid
Fibroblast
Merge

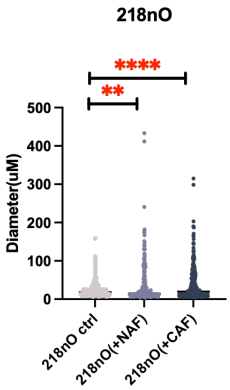
218nO
****
**
Diameter(uM)
500
400
300
200
100
0
218nO ctrl
218nO(+NAF)
218nO(+CAF)

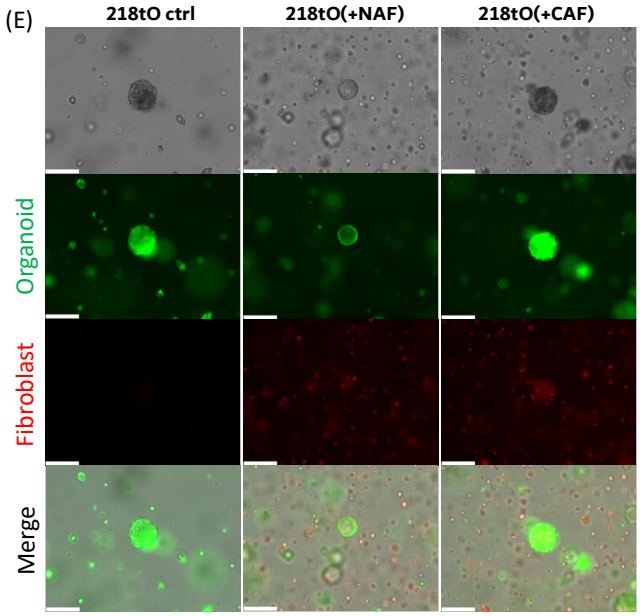
(E)
218tO ctrl
218tO(+NAF)
218tO(+CAF)
Organoid
Fibroblast
Merge

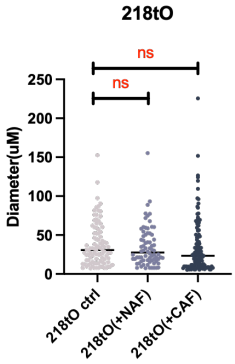
218tO
ns
ns
Diameter(uM)
250
200
150
100
50
0
218tO ctrl
218tO(+NAF)
218tO(+CAF)

Figure 2. Phenotypes of 218nO and 218tO cultured with or without fibroblast

(A) Representative images of mono- or co- cultured 218nO (Top) and 218tO (bottom) and comparison of diameter between mono-culture controls and coculture counterparts. 218nO ctrl(n=840), 218nO(+NAF), (n=3414), 218nO(+CAF), (n=2117), 218tO ctrl(n=509), 218tO(+NAF), (n=2630), 218tO(+CAF), (n=1288), scale bar=200μm.

(B) Representative EdU images of mono- or co- cultured 218nO (Left) and quantitation of area of EdU positive cells (Right).
** P-val ≤0.01, *** P-val ≤0.001,

(C) Representative EdU images of mono- or co- cultured 218tO (Left) and quantitation of area of EdU positive cells (Right).
ns, P-val>0.05

(D) Representative Celltracker images of mono- or cocultured 218nO (Left) and diameter of organoid stained by green (Right)
****P-val≤0.0001, ** P-val≤0.01

(E) Representative Celltracker images of mono- or cocultured 218tO (Left) and diameter of organoid stained by green (Right)
ns, P-val>0.05

RNA-sequencing reveals that normal and tumor organoid show distinct transcriptomic pattern

To uncover the molecular mechanism underlying difference of phenotypic changes between normal organoid and the tumor counterpart, organoids were separated, and RNA was extracted for investigation of global transcriptomic change under coculture condition. After 3 days of coculture, organoids were separated from fibroblast via centrifugal force. Successful separation of organoids was determined by qPCR validation of cell type specific genes. matched fibroblasts were used as negative control for epithelial marker and positive control for fibroblast-specific marker (Figure 3A).

Transcriptomic analysis of coculture normal and tumor organoid reveals that normal organoid showed greater change in gene expression by coculture compared to tumor organoids (Figure 3B). Total 1931 genes were up or down regulated in 218nO+218NAF coculture, and 1242 genes were up or downregulated in 218nO cocultured with matched CAF. On the other hand, there were 453 and 382 Differentially expressed genes in 218tO cultured with NAF and CAF respectively. The volcano plot also indicates significantly larger change in global transcriptome in normal organoids than tumor organoids, in response to fibroblast introduction in culture.

Gene set enrichment analysis was conducted in the purpose of verification which biological function that the DEGs contributed to (Figure 3C). Coculture of normal organoid and matched fibroblast led to activation of the epithelial-mesenchymal transition, TNFα signaling pathway and Kras signaling pathway etc. especially, genes that are related to EMT signaling pathway are known as upregulated in epithelial cell via cancer associated fibroblast[1]. In line with gene expression level, gene sets that were enriched in tumor cultured with matched fibroblast showed reduced contribution relatively to the normal counterpart (Figure 3D).

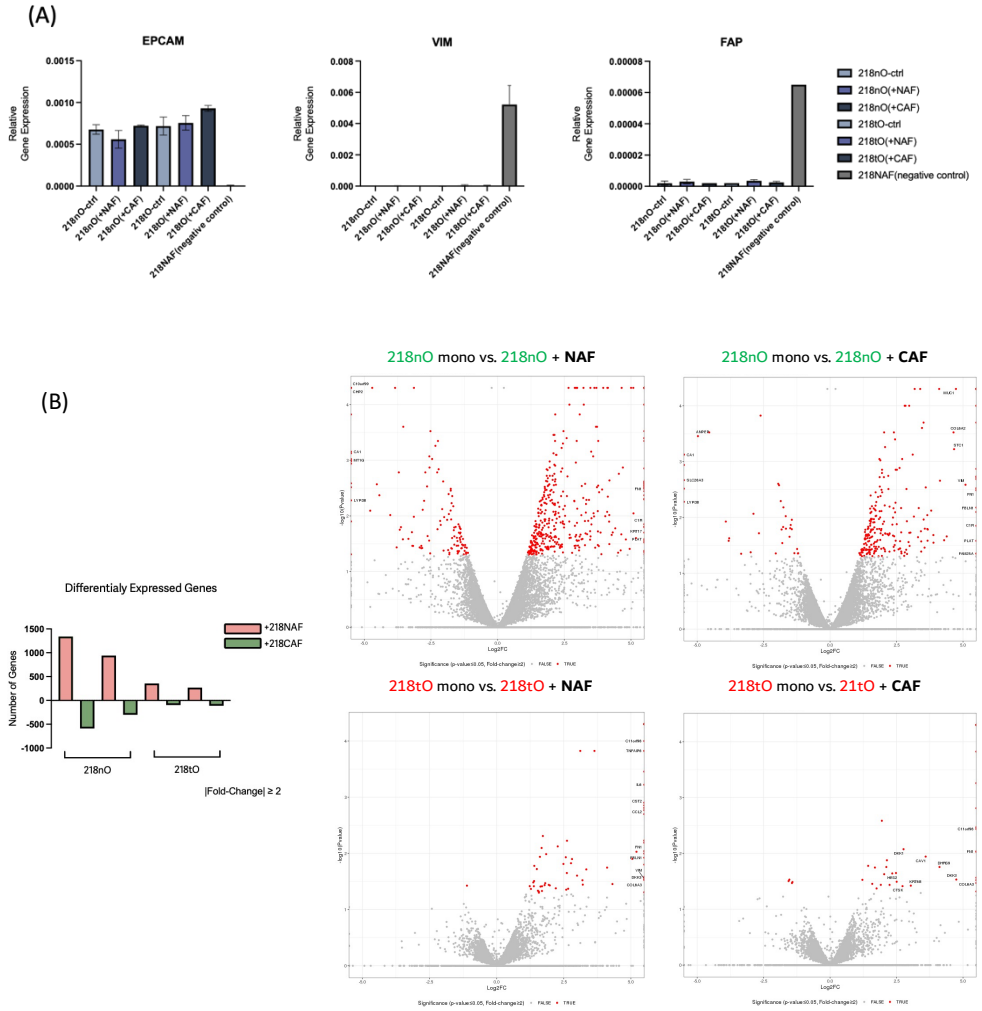
(A)
EPCAM
VIM
FAP
Relative Gene Expression
218nO-ctrl
218nO(+NAF)
218nO(+CAF)
218tO-ctrl
218tO(+NAF)
218tO(+CAF)
218NAF(negative control)
(B)
218nO mono vs. 218nO + NAF
218nO mono vs. 218nO + CAF
218tO mono vs. 218tO + NAF
218tO mono vs. 21tO + CAF
Differentialy Expressed Genes
Number of Genes
+218NAF
+218CAF
218nO
218tO
|Fold-Change| ≥ 2

(C)

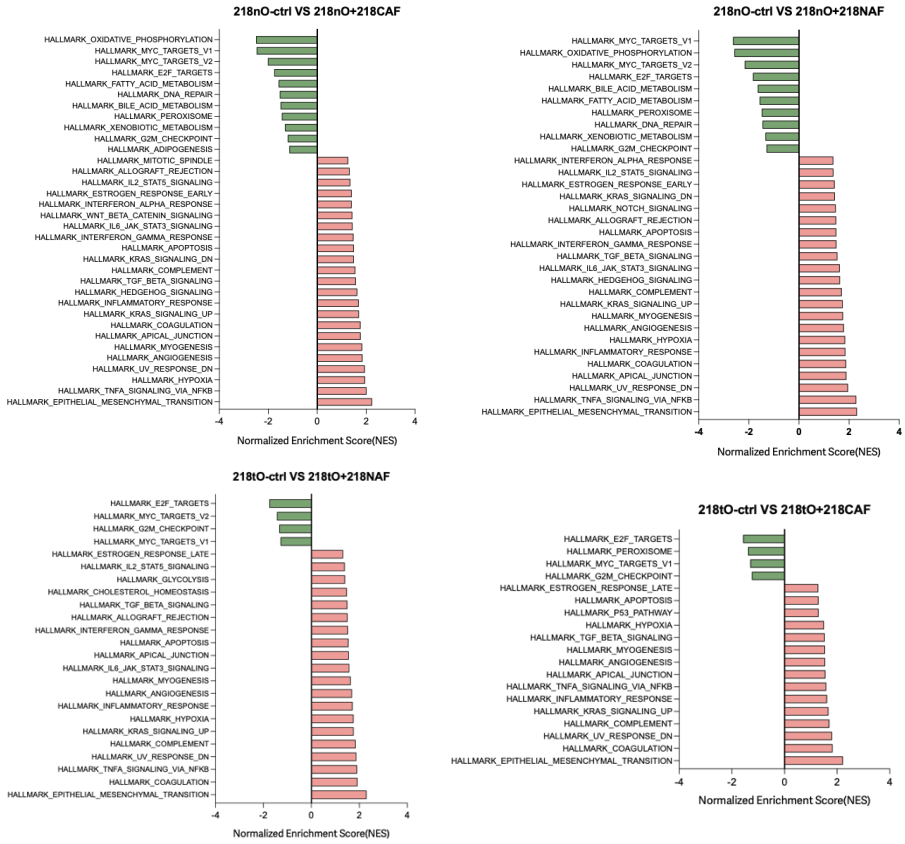
218nO-ctrl VS 218nO+218CAF
HALLMARK_OXIDATIVE_PHOSPHORYLATION
HALLMARK_MYC_TARGETS_V1
HALLMARK_MYC_TARGETS_V2
HALLMARK_E2F_TARGETS
HALLMARK_FATTY_ACID_METABOLISM
HALLMARK_DNA_REPAIR
HALLMARK_BILE_ACID_METABOLISM
HALLMARK_PEROXISOME
HALLMARK_XENOBIOTIC_METABOLISM
HALLMARK_G2M_CHECKPOINT
HALLMARK_ADIPOGENESIS
HALLMARK_MITOTIC_SPINDLE
HALLMARK_ALLOGRAFT_REJECTION
HALLMARK_IL2_STAT5_SIGNALING
HALLMARK_ESTROGEN_RESPONSE_EARLY
HALLMARK_INTERFERON_ALPHA_RESPONSE
HALLMARK_WNT_BETA_CATENIN_SIGNALING
HALLMARK_IL6_JAK_STAT3_SIGNALING
HALLMARK_INTERFERON_GAMMA_RESPONSE
HALLMARK_APOPTOSIS
HALLMARK_KRAS_SIGNALING_DN
HALLMARK_COMPLEMENT
HALLMARK_TGF_BETA_SIGNALING
HALLMARK_HEDGEHOG_SIGNALING
HALLMARK_INFLAMMATORY_RESPONSE
HALLMARK_KRAS_SIGNALING_UP
HALLMARK_COAGULATION
HALLMARK_APICAL_JUNCTION
HALLMARK_MYOGENESIS
HALLMARK_ANGIOGENESIS
HALLMARK_UV_RESPONSE_DN
HALLMARK_HYPOXIA
HALLMARK_TNFA_SIGNALING_VIA_NFKB
HALLMARK_EPITHELIAL_MESENCHYMAL_TRANSITION
-4 -2 0 2 4
Normalized Enrichment Score(NES)
218nO-ctrl VS 218nO+218NAF
HALLMARK_MYC_TARGETS_V1
HALLMARK_OXIDATIVE_PHOSPHORYLATION
HALLMARK_MYC_TARGETS_V2
HALLMARK_E2F_TARGETS
HALLMARK_BILE_ACID_METABOLISM
HALLMARK_FATTY_ACID_METABOLISM
HALLMARK_PEROXISOME
HALLMARK_DNA_REPAIR
HALLMARK_XENOBIOTIC_METABOLISM
HALLMARK_G2M_CHECKPOINT
HALLMARK_INTERFERON_ALPHA_RESPONSE
HALLMARK_IL2_STAT5_SIGNALING
HALLMARK_ESTROGEN_RESPONSE_EARLY
HALLMARK_KRAS_SIGNALING_DN
HALLMARK_NOTCH_SIGNALING
HALLMARK_ALLOGRAFT_REJECTION
HALLMARK_APOPTOSIS
HALLMARK_INTERFERON_GAMMA_RESPONSE
HALLMARK_TGF_BETA_SIGNALING
HALLMARK_IL6_JAK_STAT3_SIGNALING
HALLMARK_HEDGEHOG_SIGNALING
HALLMARK_COMPLEMENT
HALLMARK_KRAS_SIGNALING_UP
HALLMARK_MYOGENESIS
HALLMARK_ANGIOGENESIS
HALLMARK_HYPOXIA
HALLMARK_INFLAMMATORY_RESPONSE
HALLMARK_COAGULATION
HALLMARK_APICAL_JUNCTION
HALLMARK_UV_RESPONSE_DN
HALLMARK_TNFA_SIGNALING_VIA_NFKB
HALLMARK_EPITHELIAL_MESENCHYMAL_TRANSITION
-4 -2 0 2 4
Normalized Enrichment Score(NES)
218tO-ctrl VS 218tO+218NAF
HALLMARK_E2F_TARGETS
HALLMARK_MYC_TARGETS_V2
HALLMARK_G2M_CHECKPOINT
HALLMARK_MYC_TARGETS_V1
HALLMARK_ESTROGEN_RESPONSE_LATE
HALLMARK_IL2_STAT5_SIGNALING
HALLMARK_GLYCOLYSIS
HALLMARK_CHOLESTEROL_HOMEOSTASIS
HALLMARK_TGF_BETA_SIGNALING
HALLMARK_ALLOGRAFT_REJECTION
HALLMARK_INTERFERON_GAMMA_RESPONSE
HALLMARK_APOPTOSIS
HALLMARK_APICAL_JUNCTION
HALLMARK_IL6_JAK_STAT3_SIGNALING
HALLMARK_MYOGENESIS
HALLMARK_ANGIOGENESIS
HALLMARK_INFLAMMATORY_RESPONSE
HALLMARK_HYPOXIA
HALLMARK_KRAS_SIGNALING_UP
HALLMARK_COMPLEMENT
HALLMARK_UV_RESPONSE_DN
HALLMARK_TNFA_SIGNALING_VIA_NFKB
HALLMARK_COAGULATION
HALLMARK_EPITHELIAL_MESENCHYMAL_TRANSITION
-4 -2 0 2 4
Normalized Enrichment Score(NES)
218tO-ctrl VS 218tO+218CAF
HALLMARK_E2F_TARGETS
HALLMARK_PEROXISOME
HALLMARK_MYC_TARGETS_V1
HALLMARK_G2M_CHECKPOINT
HALLMARK_ESTROGEN_RESPONSE_LATE
HALLMARK_APOPTOSIS
HALLMARK_P53_PATHWAY
HALLMARK_HYPOXIA
HALLMARK_TGF_BETA_SIGNALING
HALLMARK_MYOGENESIS
HALLMARK_ANGIOGENESIS
HALLMARK_APICAL_JUNCTION
HALLMARK_TNFA_SIGNALING_VIA_NFKB
HALLMARK_INFLAMMATORY_RESPONSE
HALLMARK_KRAS_SIGNALING_UP
HALLMARK_COMPLEMENT
HALLMARK_UV_RESPONSE_DN
HALLMARK_COAGULATION
HALLMARK_EPITHELIAL_MESENCHYMAL_TRANSITION
-4 -2 0 2 4
Normalized Enrichment Score(NES)

(D)

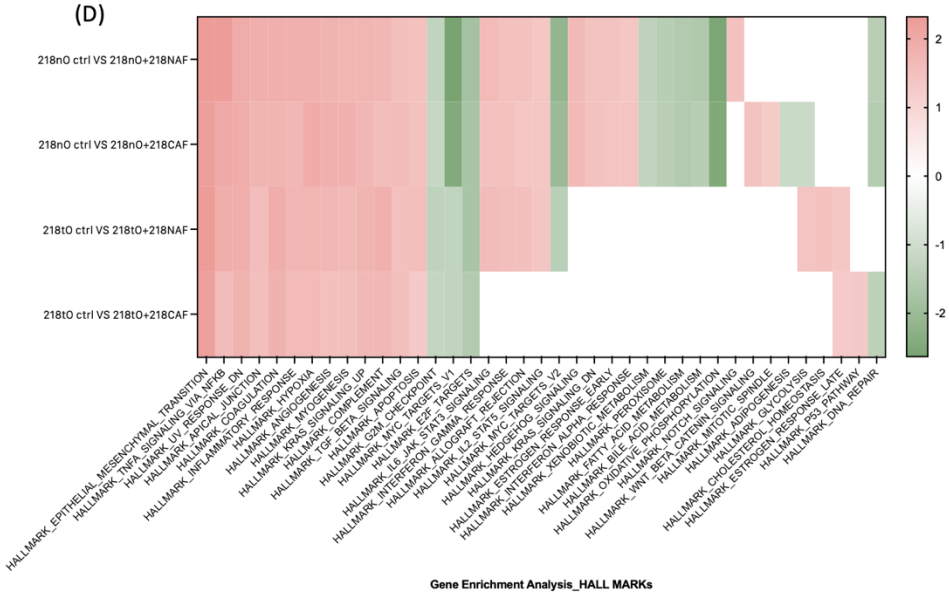
218nO ctrl VS 218nO+218NAF
218nO ctrl VS 218nO+218CAF
218tO ctrl VS 218tO+218NAF
218tO ctrl VS 218tO+218CAF
HALLMARK_EPITHELIAL_MESENCHYMAL_TRANSITION
HALLMARK_TNFA_SIGNALING_VIA_NFKB
HALLMARK_UV_RESPONSE_DN
HALLMARK_APICAL_JUNCTION
HALLMARK_INFLAMMATORY_RESPONSE
HALLMARK_COAGULATION
HALLMARK_HYPOXIA
HALLMARK_ANGIOGENESIS
HALLMARK_MYOGENESIS
HALLMARK_KRAS_SIGNALING_UP
HALLMARK_COMPLEMENT
HALLMARK_TGF_BETA_SIGNALING
HALLMARK_APOPTOSIS
HALLMARK_G2M_CHECKPOINT
HALLMARK_MYC_TARGETS_V1
HALLMARK_E2F_TARGETS
HALLMARK_IL6_JAK_STAT3_SIGNALING
HALLMARK_INTERFERON_GAMMA_RESPONSE
HALLMARK_ALLOGRAFT_REJECTION
HALLMARK_IL2_STAT5_SIGNALING
HALLMARK_MYC_TARGETS_V2
HALLMARK_HEDGEHOG_SIGNALING
HALLMARK_KRAS_SIGNALING_DN
HALLMARK_ESTROGEN_RESPONSE_EARLY
HALLMARK_INTERFERON_ALPHA_RESPONSE
HALLMARK_XENOBIOTIC_METABOLISM
HALLMARK_PEROXISOME
HALLMARK_FATTY_ACID_METABOLISM
HALLMARK_BILE_ACID_METABOLISM
HALLMARK_OXIDATIVE_PHOSPHORYLATION
HALLMARK_NOTCH_SIGNALING
HALLMARK_WNT_BETA_CATENIN_SIGNALING
HALLMARK_MITOTIC_SPINDLE
HALLMARK_ADIPOGENESIS
HALLMARK_GLYCOLYSIS
HALLMARK_CHOLESTEROL_HOMEOSTASIS
HALLMARK_ESTROGEN_RESPONSE_LATE
HALLMARK_P53_PATHWAY
HALLMARK_DNA_REPAIR
2
1
0
-1
-2
Gene Enrichment Analysis_HALL MARKs

Figure 3. Transcriptomic Analysis of 218nO,218tO cultured with or without NAF or CAF.

(A) Real-Time qPCR was conducted with primers targeting *EPCAM, VIM, FAP* and were normalized to 18S ribosomal. BAR represent the mean SD of two independent biological samples.

(B) Volcano plots of transcriptome sequencing data of 218nO ctrl, 218nO(+NAF), 218nO(+CAF), 218tO ctrl, 218tO(+NAF) and 218tO(+CAF), NAF cocultured and CAF cocultured versus mono-culture controls. Red dots indicate FDR values <0.05 and |log2(fold-change)| >1.

(C) GSEA performed on RNA sequencing data from 218nO ctrl, 218nO(+NAF), 218nO(+CAF), 218tO ctrl, 218tO(+NAF) and 218tO(+CAF). NES, normalized enrichment score. (*P*-val<0.05)

(D) Heat map showing normalized enrichment score of up- or down regulated gene set in coculture 218nO and 218tO comparing to mono-culture controls.

Comparison between transcriptome of basal normal organoid and tumor organoid shows the fundamental difference before Coculture

To confer whether the global expression regulation of organoid induced by fibroblast was due to basal variation between 218nO and 218tO. 218nO and 218tO cultured without fibroblast were subjected to EdU proliferation assay (Figure 4B). There were more EdU positive cells in 218tO comparing to 218nO, indicating that 218tO was more proliferative than 218nO under the same circumstance without fibroblast. This was a concordant resulted with known property of tumor with rapid and uncontrolled proliferation rate.

RNA-seq showed that there were 2878 genes were differentially expressed between 218nO and 218tO (Figure 4A), suggesting that innate gene expression pattern might have influence on how they were stimulated upon the stromal force. About the genes that are differentially expressed between 218nO and 218tO, 5 genes were up or downregulated in 218nO cultured with matched NAF and CAF. Notably, in the case of 218tO, there was no significance expression change upon fibroblast coculture (Figure 4C).

In summarize, normal and tumor organoid possess own transcriptomic pattern. The result suggests that this difference might have influence on transcriptional regulation by coculture of fibroblast.

(A)

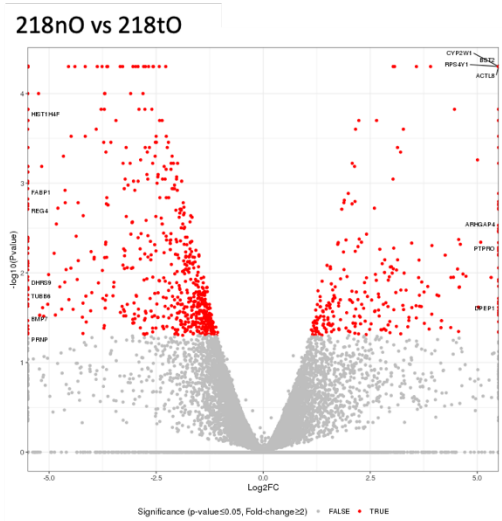

(B)

218nO ctrl

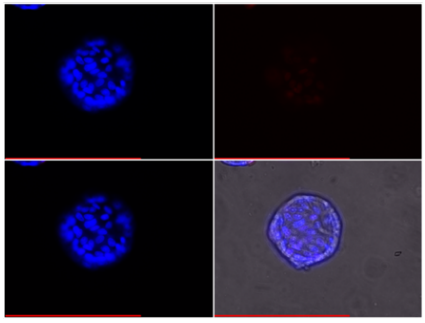

218tO ctrl

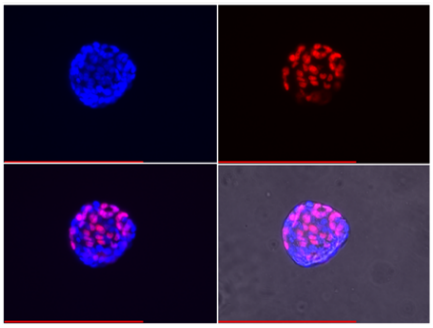

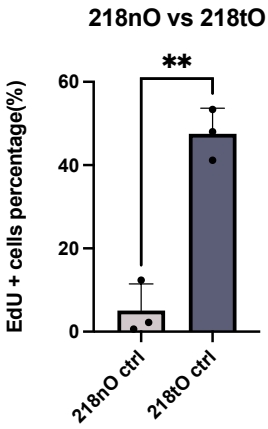

(C)

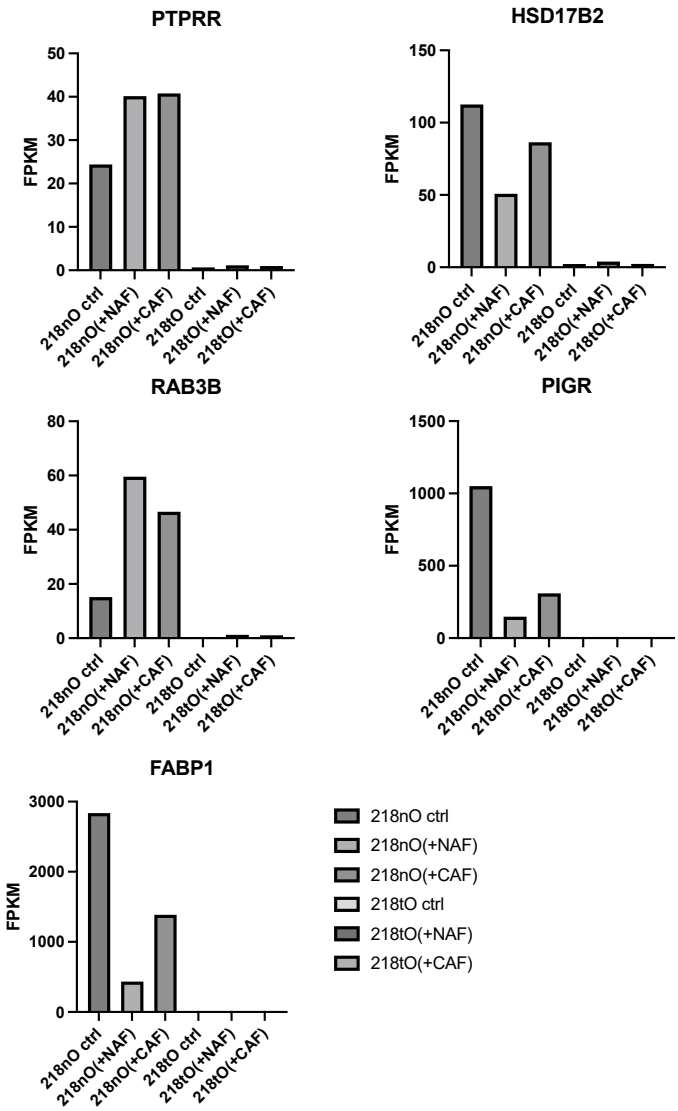
PTPRR
HSD17B2
RAB3B
PIGR
FABP1
FPKM
218nO ctrl
218nO(+NAF)
218nO(+CAF)
218tO ctrl
218tO(+NAF)
218tO(+CAF)

Figure 4. Comparison of 218nO and 218tO cultured without matched fibroblasts.

(A) Volcano plots of transcriptome sequencing data of 218nO ctrl and 218tO ctrl. Red dots indicate FDR values <0.05 and |log2(fold-change)| >1.

(B) Representative EdU images of mono-cultured 218nO and 218tO (Left), and quantitation of area of EdU positive cells (Right). ** *P*-val≤0.01

(C) mRNA expression levels of *PTPRR, HSD17B2, RAB3B, PIGR, FABP1.*

Decrease in stimulation to the tumor organoid is universal phenomenon.

To rule out the probability that down regulated response in 218 tumor organoid is the result of patient specificity, PDO and PDF from another patient 211 were cultured directly mixed with the same condition of 218 PDO and PDF. RNA was extracted and subject to RNA-seq after 3 days of coculture. Although there was some difference in degree of the number of differentially regulated Gene sets, 211nO and 218nO showed concordant result with 218 PDOs (Figure 5A).

Especially, for the genes that are related to the Epithelial-Mesenchymal Transition pathway were one of the most extensively upregulated gene sets in both 218 organoids and 211 organoids. RT-qPCR validation of RNA-seq via primers targeting 4 EMT signaling pathway genes demonstrate that 218 and 211 normal organoids were more vulnerable to stromal stimulation and showed increase significantly under coculture condition comparing to its tumor counterpart (Figure 5B). GSEA of 218 and 211 normal and tumor organoids with or without their matched fibroblast demonstrated that even if normal and tumor organoids showed enrichment in the same gene sets, the number of genes in the sets were differ. To be more specific, there were more genes in the sets that are enriched in normal and tumor organoid simultaneously (Figure 5C, D).

Altogether, these results suggested that the normal organoid and the tumor organoids react differently to supplementation of stromal components.

(A)

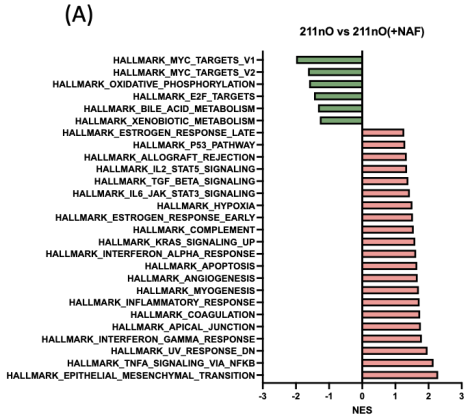
211nO vs 211nO(+NAF)
HALLMARK_MYC_TARGETS_V1
HALLMARK_MYC_TARGETS_V2
HALLMARK_OXIDATIVE_PHOSPHORYLATION
HALLMARK_E2F_TARGETS
HALLMARK_BILE_ACID_METABOLISM
HALLMARK_XENOBIOTIC_METABOLISM
HALLMARK_ESTROGEN_RESPONSE_LATE
HALLMARK_P53_PATHWAY
HALLMARK_ALLOGRAFT_REJECTION
HALLMARK_IL2_STAT5_SIGNALING
HALLMARK_TGF_BETA_SIGNALING
HALLMARK_IL6_JAK_STAT3_SIGNALING
HALLMARK_HYPOXIA
HALLMARK_ESTROGEN_RESPONSE_EARLY
HALLMARK_COMPLEMENT
HALLMARK_KRAS_SIGNALING_UP
HALLMARK_INTERFERON_ALPHA_RESPONSE
HALLMARK_APOPTOSIS
HALLMARK_ANGIOGENESIS
HALLMARK_MYOGENESIS
HALLMARK_INFLAMMATORY_RESPONSE
HALLMARK_COAGULATION
HALLMARK_APICAL_JUNCTION
HALLMARK_INTERFERON_GAMMA_RESPONSE
HALLMARK_UV_RESPONSE_DN
HALLMARK_TNFA_SIGNALING_VIA_NFKB
HALLMARK_EPITHELIAL_MESENCHYMAL_TRANSITION
-3 -2 -1 0 1 2 3
NES

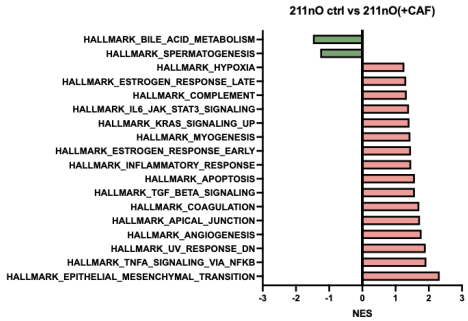
211nO ctrl vs 211nO(+CAF)
HALLMARK_BILE_ACID_METABOLISM
HALLMARK_SPERMATOGENESIS
HALLMARK_HYPOXIA
HALLMARK_ESTROGEN_RESPONSE_LATE
HALLMARK_COMPLEMENT
HALLMARK_IL6_JAK_STAT3_SIGNALING
HALLMARK_KRAS_SIGNALING_UP
HALLMARK_MYOGENESIS
HALLMARK_ESTROGEN_RESPONSE_EARLY
HALLMARK_INFLAMMATORY_RESPONSE
HALLMARK_APOPTOSIS
HALLMARK_TGF_BETA_SIGNALING
HALLMARK_COAGULATION
HALLMARK_APICAL_JUNCTION
HALLMARK_ANGIOGENESIS
HALLMARK_UV_RESPONSE_DN
HALLMARK_TNFA_SIGNALING_VIA_NFKB
HALLMARK_EPITHELIAL_MESENCHYMAL_TRANSITION
-3 -2 -1 0 1 2 3
NES

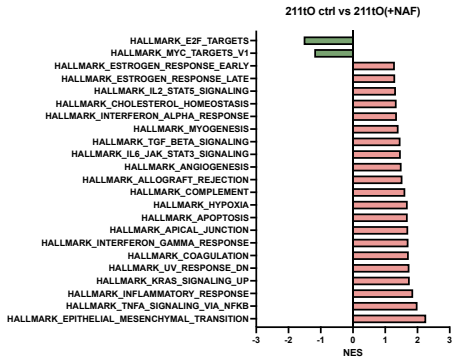
211tO ctrl vs 211tO(+NAF)
HALLMARK_E2F_TARGETS
HALLMARK_MYC_TARGETS_V1
HALLMARK_ESTROGEN_RESPONSE_EARLY
HALLMARK_ESTROGEN_RESPONSE_LATE
HALLMARK_IL2_STAT5_SIGNALING
HALLMARK_CHOLESTEROL_HOMEOSTASIS
HALLMARK_INTERFERON_ALPHA_RESPONSE
HALLMARK_MYOGENESIS
HALLMARK_TGF_BETA_SIGNALING
HALLMARK_IL6_JAK_STAT3_SIGNALING
HALLMARK_ANGIOGENESIS
HALLMARK_ALLOGRAFT_REJECTION
HALLMARK_COMPLEMENT
HALLMARK_HYPOXIA
HALLMARK_APOPTOSIS
HALLMARK_APICAL_JUNCTION
HALLMARK_INTERFERON_GAMMA_RESPONSE
HALLMARK_COAGULATION
HALLMARK_UV_RESPONSE_DN
HALLMARK_KRAS_SIGNALING_UP
HALLMARK_INFLAMMATORY_RESPONSE
HALLMARK_TNFA_SIGNALING_VIA_NFKB
HALLMARK_EPITHELIAL_MESENCHYMAL_TRANSITION
-3 -2 -1 0 1 2 3
NES

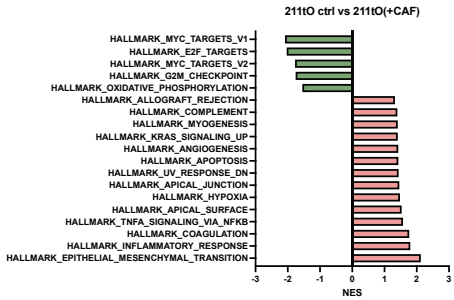
211tO ctrl vs 211tO(+CAF)
HALLMARK_MYC_TARGETS_V1
HALLMARK_E2F_TARGETS
HALLMARK_MYC_TARGETS_V2
HALLMARK_G2M_CHECKPOINT
HALLMARK_OXIDATIVE_PHOSPHORYLATION
HALLMARK_ALLOGRAFT_REJECTION
HALLMARK_COMPLEMENT
HALLMARK_MYOGENESIS
HALLMARK_KRAS_SIGNALING_UP
HALLMARK_ANGIOGENESIS
HALLMARK_APOPTOSIS
HALLMARK_UV_RESPONSE_DN
HALLMARK_APICAL_JUNCTION
HALLMARK_HYPOXIA
HALLMARK_APICAL_SURFACE
HALLMARK_TNFA_SIGNALING_VIA_NFKB
HALLMARK_COAGULATION
HALLMARK_INFLAMMATORY_RESPONSE
HALLMARK_EPITHELIAL_MESENCHYMAL_TRANSITION
-3 -2 -1 0 1 2 3
NES

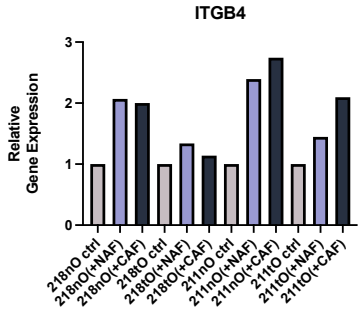
ITGB4
Relative Gene Expression
0 1 2 3
218nO ctrl
218nO(+NAF)
218nO(+CAF)
218tO ctrl
218tO(+NAF)
218tO(+CAF)
211nO ctrl
211nO(+NAF)
211nO(+CAF)
211tO ctrl
211tO(+NAF)
211tO(+CAF)

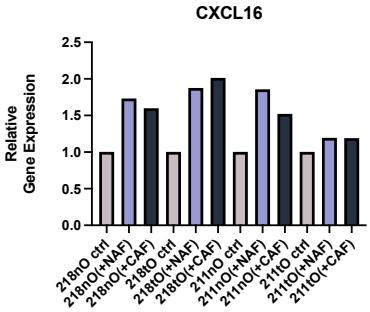
CXCL16
Relative Gene Expression
0.0 0.5 1.0 1.5 2.0 2.5
218nO ctrl
218nO(+NAF)
218nO(+CAF)
218tO ctrl
218tO(+NAF)
218tO(+CAF)
211nO ctrl
211nO(+NAF)
211nO(+CAF)
211tO ctrl
211tO(+NAF)
211tO(+CAF)

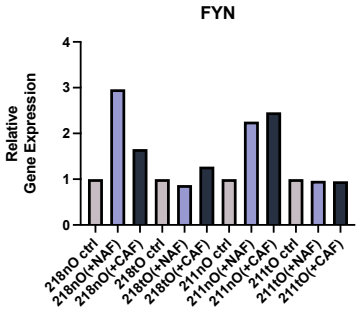
FYN
Relative Gene Expression
0 1 2 3 4
218nO ctrl
218nO(+NAF)
218nO(+CAF)
218tO ctrl
218tO(+NAF)
218tO(+CAF)
211nO ctrl
211nO(+NAF)
211nO(+CAF)
211tO ctrl
211tO(+NAF)
211tO(+CAF)

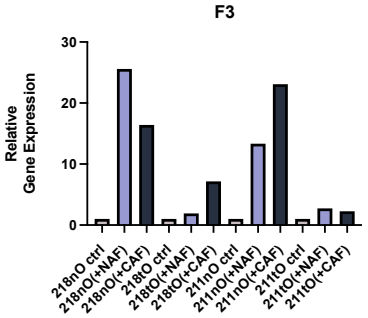
F3
Relative Gene Expression
0 10 20 30
218nO ctrl
218nO(+NAF)
218nO(+CAF)
218tO ctrl
218tO(+NAF)
218tO(+CAF)
211nO ctrl
211nO(+NAF)
211nO(+CAF)
211tO ctrl
211tO(+NAF)
211tO(+CAF)

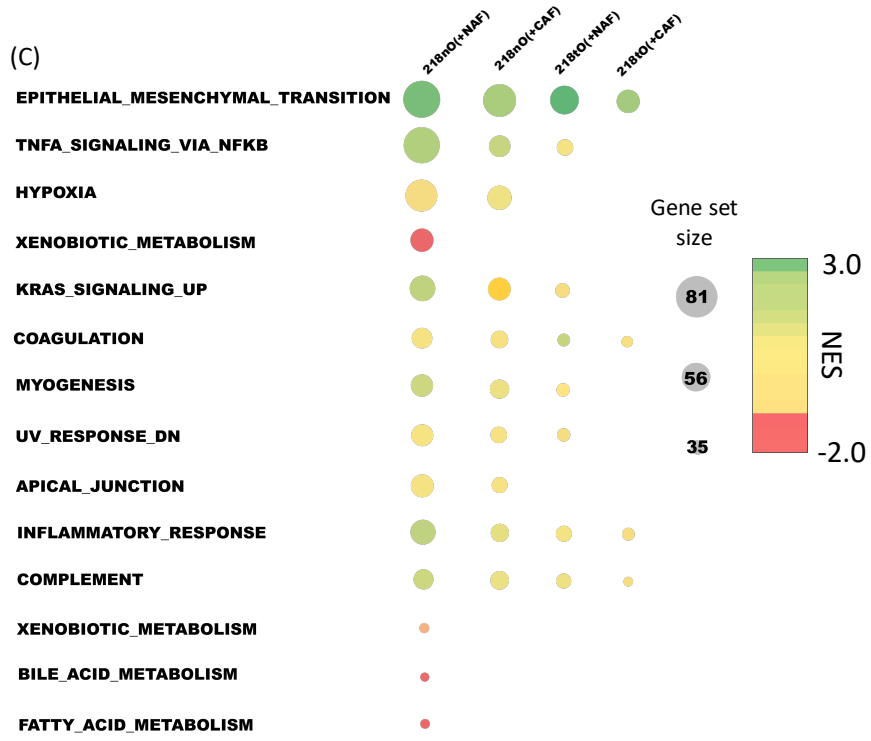
(C)
218nO(+NAF)
218nO(+CAF)
218tO(+NAF)
218tO(+CAF)
EPITHELIAL_MESENCHYMAL_TRANSITION
TNFA_SIGNALING_VIA_NFKB
HYPOXIA
XENOBIOTIC_METABOLISM
KRAS_SIGNALING_UP
COAGULATION
MYOGENESIS
UV_RESPONSE_DN
APICAL_JUNCTION
INFLAMMATORY_RESPONSE
COMPLEMENT
XENOBIOTIC_METABOLISM
BILE_ACID_METABOLISM
FATTY_ACID_METABOLISM
Gene set size
81
56
35
3.0
NES
-2.0

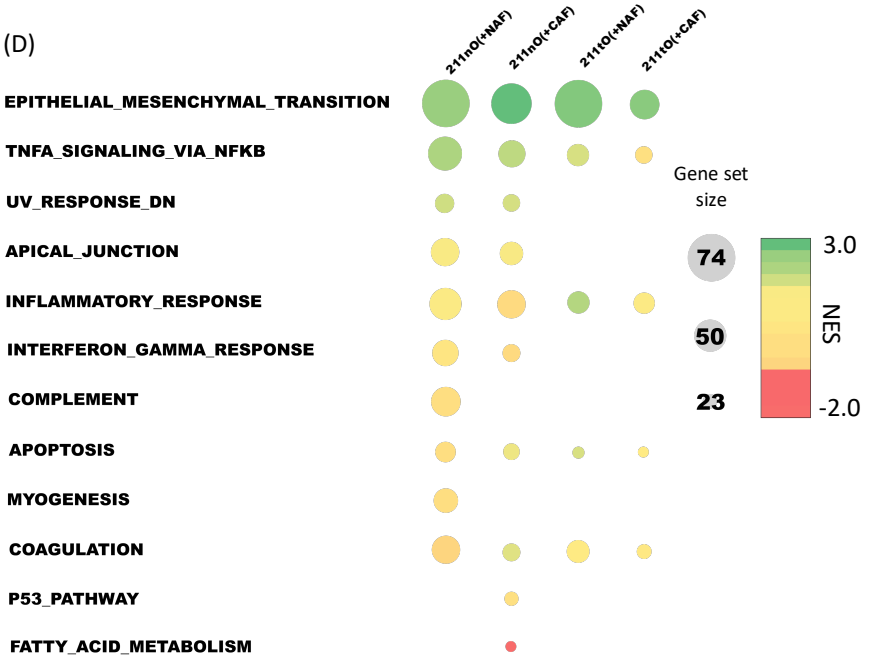
(D)
211nO(+NAF)
211nO(+CAF)
211tO(+NAF)
211tO(+CAF)
EPITHELIAL_MESENCHYMAL_TRANSITION
TNFA_SIGNALING_VIA_NFKB
UV_RESPONSE_DN
APICAL_JUNCTION
INFLAMMATORY_RESPONSE
INTERFERON_GAMMA_RESPONSE
COMPLEMENT
APOPTOSIS
MYOGENESIS
COAGULATION
P53_PATHWAY
FATTY_ACID_METABOLISM
Gene set size
74
50
23
3.0
NES
-2.0

Figure 5. Comparison of 218nO and 218tO cultured without matched fibroblasts.

(A) GSEA performed on RNA sequencing data from 211nO ctrl, 211nO(+NAF), 211nO(+CAF), 211tO ctrl, 211tO(+NAF) and 211tO(+CAF). NES, normalized enrichment score. (P-val<0.05)

(B) RT-qPCR validation with primers *targeting ITGB4, CXCL16, FYN, F3.* mRNA levels were normalized with 18s ribosomal RNA.

(C) Schematic view of common phenomenon under in-vitro coculture of 218 PDOs and PDFs. Size of the circle indicates gene set size and colors indicate Normalized Enrichment Scores (NES)

(D) Schematic view of common phenomenon under in-vitro coculture of 211 PDOs and PDFs. Size of the circle indicates gene set size and colors indicate Normalized Enrichment Scores (NES)

Discussion

In this study, Patient-Derived Organoids and its matched fibroblasts were directly mixed into the 3D Matrigel culture system, which allows these cells to interact both directly and indirectly through their cell surface receptors or cytokines. Normal colonic organoids showed phenotypic changes in coculture condition, such as increase in cell proliferation, more cystic morphology. Unlike the normal organoid, CRC organoid possess higher proliferation rate comparing to its normal counterpart. In addition, the tumor organoid showed less phenotypic changes when cultured with matched fibroblasts. To understand molecular mechanism underlying these differences, RNA-sequencing was conducted and transcriptomic pattern of normal organoid mono-culture control, normal organoid cultured with NAF or CAF, tumor organoid mono-culture control, tumor organoid cultured with NAF or CAF were compared. Interestingly, normal organoid showed numerous gene expression change and this shift occurred in less extent when it comes to tumor organoid.

It has been shown that tumorigenesis of CRC requires genetic mutations occurring spontaneously that might act as tumor-initiating force. These mutations might provide tumor with chance to accumulate more mutations and change genetic landscape that take tumor from normal counterpart. Whole Exome Sequencing (WES) will be conducted and find out whether the different transcriptomic reaction to the stromal stimulation were originated from genetic difference between normal organoid and tumor organoid.

It was revealed that Normal organoid and tumor organoid both showed induction of various signaling pathways upon their matched fibroblast coculture. It has been demonstrated that CAF provides tumor cell with advantages in tumor progression. For instance, one study showed that BRD4 ligand originated from CAF allow tumor cells to get resistance to BET inhibitor by remodeling chromatin of the cells[19]. In addition to paracrine interaction between fibroblasts and tumor cell, Direct cell-cell interaction mediated by cell surface protein might accelerate further tumor progression. Tumor cell overexpressing ATP1A1 induced NFkB signaling pathway in surrounding fibroblasts, allowing transcriptional activation of activin A, eventually lead cancer cell to activate EMT[20]. As transcriptomic pattern was widely changed under coculture condition, there might be epigenetic regulation which effects broad expression changes in cancer cell. Methylation pattern should be uncovered to verify which genomic regions showed regulated by putative transcriptional factor[14]. Chromatin immunoprecipitation Sequencing (ChiP sequencing) is a fundamental tool for identification transcription factor controlling on and off in gene expression. Chip-sequencing will be conducted to further investigate the presence of master regulator broadly affect biological processes which was induced by the stromal stimulation.

To summarize, in vitro coculture system using PDO and PDF reveals that normal epithelial and tumor cells react differently to supplementation of stromal components. Comparison of basal normal organoid and tumor organoid demonstrates that fundamental genetic background of both organoids might lead to the uncontrolled phenotypes in tumor cells. Uncovering this nature proposes a new marker to discriminate normal and tumor cells.

국문 초록

Cancer-associated fibroblast(CAF)는 고형암의 종양미세환경에서 주요한 역할을 맡고 있는 요소 중 하나로 알려져왔다. CAF 의 두가지 주요 하위 분류의 경우 종양 세포의 발달에 있어서 촉진하는 기능과 억제하는 기능이 있으며, 이는 직접 혹은 간접적인 형태로 paracrine factor 와 막 단백질을 통해 이루어진다. 이러한 상호작용은 종양 세포로 하여금 전이능, 면역 회피, 그리고 약재 내성과 같은 특징들을 얻도록 한다. 최근 연구들은 이러한 CAF 의 두가지 분류에 초점을 맞추고 있으며, 이들은 종양미세환경을 다르게 조절한다는 것이 동물 실험 모델과 세포주를 이용하여 연구가 되고 있다. 대장암의 경우 병의 초기 단계에서 유전적 돌연변이의 순차적인 발발이 주요한 촉진작용을 한다. 비교적 암의 초기 단계에서 발달을 억제한다고 알려져있는 CAF 의 역할에 대해 어떠한 방식으로 종양세포가 반응하는지에 대한 설명이 부족한 상황이다. 환자로부터 유래된 오가노이드는 환자의 특이적인 종양생물학적 특성을 그대로 반영할 것이라는 기대와 함께 최근들어서 널리 사용되고 있는 in vitro 입체 모델 시스템이다. 따라서 본 연구는 정상 상피 세포와 종양 세포가 섬유아세포의 공동 배양 아래에 어떠한 방식으로 다르게 반응하는지에 대해 초점을 두고자 한다.

환자로부터 유래한 정상 오가노이드와 종양 오가노이드, 그리고 그에 해당하는 섬유아세포가 수립된 것이 각 세포에 특이적으로 발현하는 단백질들의 발현 차이를 통해 확인되었다. 오가노이드의 경우 동일한 결과가 3 일 동안의 공동 배양 이후에도 확인되었다.

직접적인 공동배양 체계가 적용되었기 때문에 본논문에서 사용된 시스템이 세포간의 직, 간접적인 상호작용을 모두 관찰할 수 있을 것이라고 예상 하였다. 정상 오가노이드의 경우 섬유아세포와의 공동배양 이후 거시적인 형질의 변화를 보였으며 이 변화에는 세포의 분열 촉진에 의한 직경증가와 낭포와 같은 모양의 증가가 해당된다.

반면 종양 오가노이드의 경우 정상 오가노이드보다 섬유아세포와의 공동배양 이후 뚜렷한 형질적인 차이를 보이지 않았다.

이러한 정상 오가노이드와 종양 오가노이드간의 유의미한 차이가 어떠한 분자적 체제에 의한 결과인지 확인하고자 RNA-시퀀싱이 진행되었으며 추가적인 분석을 위하여 Gene Set Enrichment Analysis 가 진행되었다. 이를 통해 정상 오가노이드의 경우, 섬유아세포와 공동배양하였을 때 종양 오가노이드에 비해 상대적으로 다양한 기전과 관련된 유전자들이 증가되거나 감소하는 정도가 큰 것을 확인 할 수 있었다. 같은 결과가 다른 환자로 부터 얻은 샘플에서도 반복되었다.

모든 결과를 종합하였을 때, in vitro 에서 환자유래 오가노이드와 섬유아세포를 이용한 공동배양 시스템이 in vivo 의 종양미세환경을 구현하고, 정상 오가노이드와 종양 오가노이드가 섬유아세포와의 배양에 대해 서로 분자적, 형질적으로 다르게 반응하도록 하는 전사적 기제가 새로운 바이오마커가 될 수 있음을 기대한다.

주요어 : 대장암, 종양미세환경, 환자 유래 오가노이드, 환자 유래 섬유아세포, CAF, NAF

학 번 : 2020-29330

Reference

1 Biffi, G. & Tuveson, D. A. Diversity and Biology of Cancer-Associated Fibroblasts. *Physiol Rev* **101**, 147-176, doi:10.1152/physrev.00048.2019 (2021).

2 Cho, Y. W. *et al.* Patient-derived organoids as a preclinical platform for precision medicine in colorectal cancer. *Mol Oncol* **16**, 2396-2412, doi:10.1002/1878-0261.13144 (2022).

3 Costea, D. E., Johannessen, A. C. & Vintermyr, O. K. Fibroblast control on epithelial differentiation is gradually lost during in vitro tumor progression. *Differentiation* **73**, 134-141, doi:DOI 10.1111/j.1432-0436.2005.00017.x (2005).

4 Davidson, S. *et al.* Fibroblasts as immune regulators in infection, inflammation and cancer. *Nat Rev Immunol* **21**, 704-717, doi:10.1038/s41577-021-00540-z (2021).

5 Drost, J. *et al.* Sequential cancer mutations in cultured human intestinal stem cells. *Nature* **521**, 43-47, doi:10.1038/nature14415 (2015).

6 Gerling, M. *et al.* Stromal Hedgehog signalling is downregulated in colon cancer and its restoration restrains tumour growth (vol 7, 12321, 2016). *Nat Commun* **7**, doi:ARTN 12936 10.1038/ncomms12936 (2016).

7 Goulet, C. R. *et al.* Cancer-associated fibroblasts induce epithelial-mesenchymal transition of bladder cancer cells through paracrine IL-6 signalling. *Bmc Cancer* **19**, doi:ARTN 137 10.1186/s12885-019-5353-6 (2019).

8 Guinney, J. *et al.* The consensus molecular subtypes of colorectal cancer. *Nat Med* **21**, 1350-1356, doi:10.1038/nm.3967 (2015).

9 Ito, Y. *et al.* Lung fibroblasts accelerate wound closure in human alveolar epithelial cells through hepatocyte growth factor/c-Met signaling. *Am J Physiol-Lung C* **307**, L94-L105, doi:10.1152/ajplung.00233.2013 (2014).

10 Kim, J. I. *et al.* A highly annotated whole-genome sequence of a Korean individual (Reprinted from Nature, vol 460, pg 1011-1015, 2009). *Nat Genet*, S2-S6 (2009).

11 Kobayashi, H. *et al.* Cancer-associated fibroblasts in gastrointestinal cancer. *Nat Rev Gastroenterol Hepatol* **16**, 282-295, doi:10.1038/s41575-019-0115-0 (2019).

12 Lee, J. J. *et al.* Control of inflammation by stromal Hedgehog pathway activation restrains colitis. *Proc Natl Acad Sci U S A* **113**, E7545-E7553, doi:10.1073/pnas.1616447113 (2016).

13 Ganesh, K. *et al.* L1CAM defines the regenerative origin of metastasis-initiating cells in colorectal cancer (vol 1, pg 28, 2020). *Nat Cancer* **1**, 1128-1128, doi:10.1038/s43018-020-00130-3 (2020).
14 Moore, L. D., Le, T. & Fan, G. P. DNA Methylation and Its Basic Function. *Neuropsychopharmacol* **38**, 23-38, doi:10.1038/npp.2012.112 (2013).
15 Rodrigues, J., Heinrich, M. A., Teixeira, L. M. & Prakash, J. 3D In Vitro Model (R)evolution: Unveiling Tumor-Stroma Interactions. *Trends Cancer* **7**, 249-264, doi:10.1016/j.trecan.2020.10.009 (2021).
16 Lin, S. *et al.* Comparison of the transcriptional landscapes between human and mouse tissues. *P Natl Acad Sci USA* **111**, 17224-17229, doi:10.1073/pnas.1413624111 (2014).
17 Yun, J. *et al.* Reduced cohesin destabilizes high-level gene amplification by disrupting pre-replication complex bindings in human cancers with chromosomal instability. *Nucleic Acids Res* **44**, 558-572, doi:10.1093/nar/gkv933 (2016).
18 Subramanian, A. *et al.* Gene set enrichment analysis: A knowledge-based approach for interpreting genome-wide expression profiles. *P Natl Acad Sci USA* **102**, 15545-15550, doi:10.1073/pnas.0506580102 (2005).
19 Wang, W. Y. *et al.* Stromal induction of BRD4 phosphorylation Results in Chromatin Remodeling and BET inhibitor Resistance in Colorectal Cancer. *Nat Commun* **12**, doi:ARTN 4441 10.1038/s41467-021-24687-4 (2021).
20 Chen, Y. I. *et al.* Homophilic ATP1A1 binding induces activin A secretion to promote EMT of tumor cells and myofibroblast activation. *Nat Commun* **13**, doi:ARTN 2945 10.1038/s41467-022-30638-4 (2022).